Molecular dynamics integration and molecular vibrational theory. III. The infrared spectrum of water

Matej Praprotnik and Dušanka Janežič[a)]
National Institute of Chemistry, Hajdrihova 19, 1000 Ljubljana, Slovenia

(Received 17 November 2004; accepted 11 February 2005; published online 29 April 2005)

The new symplectic molecular dynamics (MD) integrators presented in the first paper of this series were applied to perform MD simulations of water. The physical properties of a system of flexible TIP3P water molecules computed by the new integrators, such as diffusion coefficients, orientation correlation times, and infrared (IR) spectra, are in good agreement with results obtained by the standard method. The comparison between the new integrators' and the standard method's integration time step sizes indicates that the resulting algorithm allows a 3.0 fs long integration time step as opposed to the standard leap-frog Verlet method, a sixfold simulation speed-up. The accuracy of the method was confirmed, in particular, by computing the IR spectrum of water in which no blueshifting of the stretching normal mode frequencies is observed as occurs with the standard method. © *2005 American Institute of Physics*. [DOI: 10.1063/1.1884609]

I. INTRODUCTION

Molecular dynamics (MD) simulations are among the main theoretical methods of investigating complex molecular systems, e.g., water.[1] In recent years, MD simulations have provided a substantial amount of data about water structural and dynamical properties.[2–9] In the MD simulation, the classical equations of motion for an assembly of interacting particles are solved, usually numerically. However, computing time is a serious handicap in this regard. Several MD integration approaches were derived[10–16] to overcome this problem. The most used is the symplectic second-order leap-frog Verlet (LFV) method.[17] Using this method, a water system of flexible TIP3P water molecules[18,19] can be accurately integrated by 0.5 fs integration time step.

Water plays a unique role among liquids due to its ubiquity, importance for life, and also anomalous liquid properties. Therefore it represents one of the most interesting and challenging systems to study for the MD simulation. The MD simulations of liquid water have been hindered by the short time step allowed by integration methods[1,20] owing to strong intramolecular and intermolecular interactions in the system, which generate atom motion on a very short time scale (femtosecond). New semianalytical symplectic MD integrators introduced in the first paper of this series,[21] however, allow the use of longer time steps owing to the analytical treatment of high-frequency molecular vibrations.

Our newly developed MD integrators are different to other approaches, which also allow longer time steps,[12–16] in that we split the whole Hamiltonian of the system into two parts corresponding to the fast and slow molecular motions, respectively, and that the high-frequency molecular motions, i.e., vibrations, are resolved analytically by normal coordinates. This approach allows using a long MD integration time step and also accurate calculations of the physical properties of the system.

In this paper we present a series of MD simulations of a water system of flexible TIP3P water molecules[18,19] using new integrators[21] with a long integration time step to successfully reproduce liquid water's structual and dynamical properties at 300 K. Results show that the new integrators allow an integration time step up to six times longer than the standard leap-frog Verlet method and are especially efficient for calculating the vibrational IR spectra because of their analytical treatment of high-frequency molecular vibrations.

II. METHODS

A. Overview of integration methods

A series of MD simulations of planar water molecules using the new MD integrators described in the first paper of this series[21] were performed. The newly developed integrator SISM and its three derivates [multiple time stepping SISM (SISM-MTS), equilibrium SISM (SISM-EQ), equilibrium SISM-MTS (SISM-MTS-EQ)] (Ref. 21) are explicit second-order symplectic methods, which enables them to resolve the equations of motion, in part analytically, with a long integration time step. These methods, derived within the Lie group theory,[22] are especially suitable to compute the IR spectra of systems of flexible molecules with one equilibrium configuration and no internal rotation, e.g., water molecules. As reference methods the LFV and LFV-EQ (Ref. 21) were chosen because they are a time reversible symplectic second-order methods with only one variable parameter—the integration time step size.

B. Diffusion coefficient

The diffusion coefficient, which characterizes translational motion of water molecules, is defined as[1]

[a)]Author to whom correspondence should be addressed. Electronic mail: dusa@cmm.ki.si

$$D = \frac{1}{3}\int_0^\infty C(t)dt, \tag{1}$$

where $C(t)$ is the oxygen velocity autocorrelation function,

$$C(t) = \langle \mathbf{v}_i(t) \cdot \mathbf{v}_i(0)\rangle = \frac{1}{Mm}\sum_{k=1}^{M}\sum_{i=1}^{m} \mathbf{v}_i(t_k) \cdot \mathbf{v}_i(t_k + t) \tag{2}$$

and $\mathbf{v}_i(t)$ the velocity of the oxygen atom in the ith molecule at time t. Angular brackets denote the average over all m oxygens and all M time origins.[23] The diffusion coefficient (1) is, in the long time limit, equal to the corresponding diffusion coefficients calculated either from the hydrogen velocity autocorrelation function or water molecule's center-of-mass velocity autocorrelation function.[2]

The diffusion coefficient can be also calculated from the displacements of oxygen atoms using the Einstein relation[23]

$$D = \frac{1}{3}\lim_{t\to\infty}\frac{\langle|\mathbf{r}_i(t) - \mathbf{r}_i(0)|^2\rangle}{2t}, \tag{3}$$

where $\mathbf{r}_i(t)$ is the position of the oxygen atom in the ith water molecule at time t and averaging is performed over all oxygen atoms and all choices of time origin. Also, in the long time limit, the diffusion coefficient determined in this way is equal to the corresponding diffusion coefficients calculated either from the trajectory of the hydrogen atoms or the trajectory of the water molecules' centers of mass.[2]

C. Orientational correlation times

Rotational motion of the molecules is described by single molecule orientational autocorrelation functions[1,24] of the corresponding intramolecular vectors

$$C_l^\alpha(t) = \langle P_l(\mathbf{n}^\alpha(t) \cdot \mathbf{n}^\alpha(0))\rangle, \tag{4}$$

where P_l is the lth degree Legendre polynomial and $\mathbf{n}^\alpha$ is a unit vector pointing along the α axis in the internal coordinate system of an individual molecule.[2,25] In our study we have used three different α axes: the α=HH axis points along the vector connecting two hydrogen atoms in a water molecule; the $\alpha=\mu$ axis points along the dipole moment of a water molecule; and the $\alpha=\perp$ axis points along the direction perpendicular to the molecular plane.

Single molecule correlation times can be determined by writing the functions (4) in the form

$$C_l^\alpha(t) = \exp(-t/\tau_l^\alpha), \tag{5}$$

where τ_l^α is the corresponding correlation time[1,25] In the present work, the correlation times τ_l^α were determined from $\ln C_l^\alpha(t)$ in the time interval from 1.0 ps to 2.0 ps by the linear regression method.[26]

D. IR spectrum

The infrared (IR) absorption spectrum is obtained by Fourier transformation of the dipole moment autocorrelation function as[23,27,28]

$$I(\omega) \propto \int_0^\infty \langle \mathbf{M}(t) \cdot \mathbf{M}(0)\rangle \cos(\omega t)dt, \tag{6}$$

where $I(\omega)$ is the spectral density, $\mathbf{M}(t)$ is the total dipole moment of the system at time t, and ω is the vibration frequency. $\mathbf{M}(t)$ is equal to the sum of all the individual dipole moments of the molecules in the simulation box[23,27]

$$\mathbf{M}(t) = \sum_{i=1}^{m} \boldsymbol{\mu}_i(t), \tag{7}$$

where $\boldsymbol{\mu}_i(t)$ is the dipole moment of the ith molecule at time t and m is the number of molecules in the simulation box. The autocorrelation function of the dipole moment is given by[29,30]

$$\langle \mathbf{M}(t) \cdot \mathbf{M}(0)\rangle = \left\langle \sum_{j=1}^{n} e_j \mathbf{r}_j(t) \cdot \sum_{j=1}^{n} e_j \mathbf{r}_j(0) \right\rangle, \tag{8}$$

where n is the number of all the atoms in the system, e_j is the fixed electric charge of the jth atom, and $\mathbf{r}_j(t)$ is the position vector of the jth atom at time t. The angular brackets represent an average taken over all time origins. The IR spectrum can be also obtained using the electrical flux-flux autocorrelation function

$$\begin{aligned}\left\langle \sum_{j=1}^{n} e_j \mathbf{v}_j(t) \cdot \sum_{j=1}^{n} e_j \mathbf{v}_j(0) \right\rangle &= \left\langle \sum_{j=1}^{n} e_j \frac{d\mathbf{r}_j(t)}{dt} \cdot \sum_{j=1}^{n} e_j \frac{d\mathbf{r}_j(0)}{dt} \right\rangle \\ &= \left\langle \frac{d\mathbf{M}(t)}{dt} \cdot \frac{\mathbf{M}(0)}{dt} \right\rangle,\end{aligned} \tag{9}$$

which corresponds the autocorrelation function of the time derivative of the dipole moment.[29,30] The spectral density is then calculated as[29–31]

$$\begin{aligned}I(\omega) &\propto \int_0^\infty \left\langle \frac{d\mathbf{M}(t)}{dt} \cdot \frac{d\mathbf{M}(0)}{dt} \right\rangle \cos(\omega t)dt \\ &= \int_0^\infty \left\langle \sum_{j=1}^{n} e_j \mathbf{v}_j(t) \cdot \sum_{j=1}^{n} e_j \mathbf{v}_j(0) \right\rangle \cos(\omega t)dt.\end{aligned} \tag{10}$$

Since the calculated IR spectrum using Eq. (10) differs from the IR spectrum obtained by Eq. (6) only by its intensity,[29] we have used Eq. (10) in our work for calculating the IR spectrum.

III. COMPUTATIONAL DETAILS

As a representative from the class of the planar molecules, for which the SISM is most efficient, we have picked the water (H_2O) molecule. The equilibrium configuration is depicted in Fig. 1, in which atoms 1 and 3 denote hydrogen atoms and atom 2 denotes the oxygen atom in the H_2O molecule.

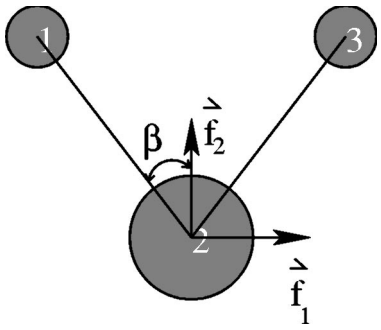

FIG. 1. Description of the positions of atoms in the equilibrium configuration of a water molecule. The orthogonal unit vectors $\mathbf{f}_1$ and $\mathbf{f}_2$ are the two unit vectors, which define the internal coordinate system of a molecule.

A. Water model

We have chosen the flexible TIP3P model[18] as the model for the water molecule. The original TIP3P model is changed in such a way that it allows for the flexibility of bonds and angles and also each of the hydrogens was given a small van der Waals radius to prevent the "electrostatic catastrophe" at small distances between water molecules.[19,32]

The model Hamiltonian is[18,19]

$$H = \sum_i \frac{\mathbf{p}_i^2}{2m_i} + \frac{1}{2}\sum_{\text{bonds}} k_b(b-b_0)^2 + \frac{1}{2}\sum_{\text{angles}} k_\theta(\theta-\theta_0)^2 + \sum_{i>j}\frac{e_i e_j}{4\pi\epsilon_0 r_{ij}} + \sum_{i>j} 4\varepsilon_{ij}\left[\left(\frac{\sigma_{ij}}{r_{ij}}\right)^{12} - \left(\frac{\sigma_{ij}}{r_{ij}}\right)^{6}\right], \tag{11}$$

where i and j run over all atoms, m_i is the mass of the ith atom, $\mathbf{p}_i = m_i\mathbf{v}_i$ is the linear momentum of the ith atom, b_0 and θ_0 are reference values for bond lengths and angles, respectively, k_b and k_θ are corresponding force constants, e_i denotes the charge on the ith atom, ϵ_0 is the dielectric constant in vacuum, r_{ij} is the distance between the ith and jth atoms, and ε_{ij} and σ_{ij} are the corresponding constants of the Lennard-Jones potential. The van der Waals and Coulomb interactions between the atoms of the same molecule are not calculated explicitly because they are already taken into account by the bond stretching and angle bending terms in the Hamiltonian (11). The parameters of the model are given in Table I.

TABLE I. Parameters of the flexible TIP3P model of the H_2O molecule (Refs. 18 and 19). The quantity e_0 is the elementary charge.

Parameter	Value
$b_{\mathrm{OH}_0} = b_0$	0.9572 Å
θ_0	104.52°
$k_{b_{\mathrm{OH}}} = k_b$	900.0 kcal/mol/Å^2
k_θ	110.0 kcal/mol/rad^2
$e_{\mathrm{H}_1} = e_1$	$0.417e_0$
$e_{\mathrm{O}} = e_2$	$-0.834e_0$
$e_{\mathrm{H}_2} = e_3$	$0.417e_0$
σ_{OO}	3.1507 Å
σ_{HH}	0.40 Å
ϵ_{OO}	−0.152 073 kcal/mol
ϵ_{HH}	−0.045 98 kcal/mol

B. Vibrational potential energy and internal coordinate system

The vibrational potential energy is the sum of the vibrational potential energies of all of the molecules in the system

$$V_{vib} = \sum_{k=1}^{m} V_{vib_k} = \frac{1}{2}\sum_{bonds} k_b(b-b_0)^2 + \frac{1}{2}\sum_{angles} k_\theta(\theta-\theta_0)^2, \tag{12}$$

where V_{vib_k} is the vibrational potential energy of the kth molecule in the system and m is the number of molecules in the system.

The potential function V_{harm}, which is developed from Eq. (12) in the same way as in the previous paper,[33] is

$$V_{harm} = V_{stretch} + V_{bend}, \tag{13}$$

where $V_{stretch}$ and V_{bend} are quadratic potential functions in terms of relative Cartesian displacement coordinates, which represent the harmonic approximations for the bond stretching and angle bending potentials, respectively.[21] The expressions for $V_{stretch}$ and V_{bend} are obtained by projecting the displacements of atoms along and perpendicular to the bonds between the atoms in each molecule.[34]

$V_{stretch}$ is then

$$\begin{aligned} V_{stretch} &= \tfrac{1}{2}k_b[((\Delta x_1 - \Delta x_2, \Delta y_1 - \Delta y_2, \Delta z_1 - \Delta z_2) \\ &\quad \cdot (-\sin\beta, \cos\beta, 0)^T)^2 + ((\Delta x_3 - \Delta x_2, \Delta y_3 \\ &\quad - \Delta y_2, \Delta z_3 - \Delta z_2) \cdot (\sin\beta, \cos\beta, 0)^T)^2] \\ &= \tfrac{1}{2}k_b[[-(\Delta x_1 - \Delta x_2)\sin\beta + (\Delta y_1 - \Delta y_2)\cos\beta]^2 \\ &\quad + [(\Delta x_3 - \Delta x_2)\sin\beta + (\Delta y_3 - \Delta y_2)\cos\beta]^2] \end{aligned} \tag{14}$$

and V_{bend} is

$$\begin{aligned} V_{bend} &= \frac{1}{2}k_\theta\left[\frac{1}{b_0}[(\Delta x_1 - \Delta x_2, \Delta y_1 - \Delta y_2, \Delta z_1 - \Delta z_2) \right. \\ &\quad \cdot (-\cos\beta, -\sin\beta, 0)^T] + \frac{1}{b_0}[(\Delta x_3 - \Delta x_2, \Delta y_3 \\ &\quad \left. - \Delta y_2, \Delta z_3 - \Delta z_2) \cdot (\cos\beta, -\sin\beta, 0)]\right]^2 \\ &= \frac{1}{2}k_\theta\left[\frac{1}{b_0}[-(\Delta x_1 - \Delta x_2)\cos\beta - (\Delta y_1 - \Delta y_2)\sin\beta \right. \\ &\quad \left. + (\Delta x_3 - \Delta x_2)\cos\beta - (\Delta y_3 - \Delta y_2)\sin\beta]\right]^2 \\ &= \frac{1}{2}\frac{k_\theta}{b_0^2}[(\Delta x_3 - \Delta x_1)\cos\beta \\ &\quad + (2\Delta y_2 - \Delta y_1 - \Delta y_3)\sin\beta]^2. \end{aligned} \tag{15}$$

The vibrational frequencies corresponding to normal modes of vibration of the flexible TIP3P water model[18,19] are obtained in the same way as in the previous paper[33] and are reported in Table II. We checked the accuracy of vibrational frequencies numerically obtained in this way with the corresponding analytically computed vibrational frequencies.[34]

TABLE II. Experimental vibrational frequencies of the H_2O molecule (Ref. 47) and normal mode frequencies of the H_2O molecule determined by normal mode analysis using parameters from Table I.

Normal mode	$1/\lambda$ (cm^{-1}) (experiment)[a]	$1/\lambda$ (cm^{-1}) (theory)[b]
Antisymmetric O–H stretch	3756	3381
Symmetric O–H stretch	3652	3334
Angle bending	1595	1743

[a]Experimental vibrational frequencies.
[b]Normal mode frequencies.

The moving internal coordinate system is for each molecule in the system defined with the same procedure as in the previous paper.[33] The elements of the matrix $\mathcal{F}^{-1/2}$, which is required to determine the unit vectors of the internal coordinate system of a molecule in the SISM,[21] are explicitly written as

$$\mathcal{F}^{-1/2}(1,1) = \frac{d + \mathcal{F}(2,2)}{ds}, \tag{16}$$

$$\mathcal{F}^{-1/2}(2,2) = \frac{d + \mathcal{F}(1,1)}{ds}, \tag{17}$$

$$\mathcal{F}^{-1/2}(1,2) = -\frac{\mathcal{F}(1,2)}{ds}, \tag{18}$$

$$\mathcal{F}^{-1/2}(2,1) = \mathcal{F}^{-1/2}(1,2), \tag{19}$$

where $d = \sqrt{\mathcal{F}(1,1)\mathcal{F}(2,2) - \mathcal{F}(1,2)^2}$ and $s = \sqrt{2d + \mathcal{F}(1,1) + \mathcal{F}(2,2)}$.[35]

C. Simulation protocol

All MD calculations are carried out for the system of 256 flexible TIP3P water molecules at the system density $\rho = 1.0\ \mathrm{g/cm^3}$ and $T = 300$ K. The corresponding simulation box size is $a = 19.7$ Å. Periodic boundary conditions are imposed to overcome the problem of surface effects; the minimum image convention is used.[1] The Coulomb interactions are truncated using the force-shifted potential[36] at a cut-off distance $r_{off} = 8.5$ Å.[37] The Lennard-Jones interactions are shifted by adding the term $C_{ij} r_{ij}^6 + D_{ij}$ to the potential, where C_{ij} and D_{ij} are chosen such that the potential and force are zero at $r_{ij} = r_{off}$.[19] The initial positions and velocities of the atoms are chosen at random. The system is then equilibrated for 20 ps, where the velocities are scaled every 500 integration steps to correspond to a temperature of 300.0 K. Afterwards an additional 30 ps of equilibration is carried out at the constant total energy of the system so that the velocity corresponds to the Maxwell distribution at 300 K. Simulations are then performed for 100 ps using different integrators and/or integration time steps.

IV. RESULTS AND DISCUSSION

As in the previous paper[33] the error in total energy $\Delta E/E$ defined as

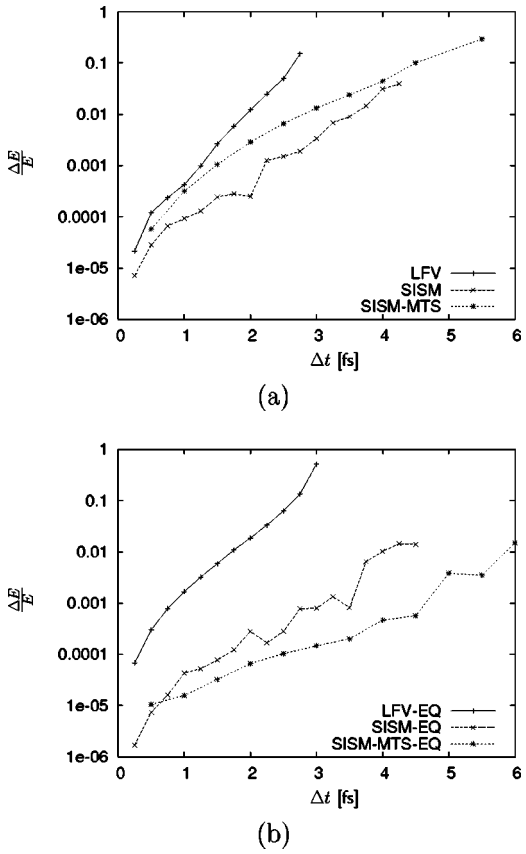

FIG. 2. (a) Error in the total energy of the system of 256 water molecules with $\rho = 1.0\ \mathrm{g/cm^3}$ at $T = 300$ K using the LFV, SISM, and SISM-MTS for $M = 1000$. (b) Error in total energy of the system of 256 water molecules with $\rho = 1.0\ \mathrm{g/cm^3}$ at $T = 300$ K using the LFV-EQ, SISM-EQ, and SISM-MTS-EQ for $M = 1000$.

$$\frac{\Delta E}{E} = \frac{1}{M}\sum_{k=1}^{M}\left|\frac{E_0 - E_k}{E_0}\right|, \tag{20}$$

where E_0 is the initial energy, E_k is the total energy of the system at the integration step k, and M is the total number of integration steps, was monitored for all methods.

In Fig. 2(a), in which the error in total energy for the system of water molecules for the LFV, SISM, and SISM-MTS is displayed, it can be observed that the error in total energy for a 1.25 fs integration time step for the SISM corresponds to the same error as for the 0.5 fs integration time step for the LFV. The estimated value for the maximal acceptable integration time step for the LFV is 0.5 fs since the period of the antisymmetric bond stretching is equal to 9.9 fs (see Table II). This means that for the same level of accuracy, the SISM allows the use of up to a two and a half times longer integration time step than the LFV. The jump in the error in total energy, which can be observed in Fig. 2(a) for a 2.5 fs integration time step, can possibly be explained by nonlinear instabilities occurring when the integration step size is a fourth of the period of the fastest stretching vibrations in water molecules.[38]

For the system of water molecules, a high amount of anharmonic forces occurs due to the strong anharmonic potential describing the interactions in the system. However, as in the case of the hydrogen peroxide simulation,[33] the SISM-

TABLE III. Comparison of $g_{OO}(r)$, $g_{OH}(r)$, and $g_{HH}(r)$ calculated by the LFV, SISM, and SISM-MTS. We give the positions and heights of the first maximum of the calculated functions and the corresponding experimental values (Ref. 42).

	LFV (0.5 fs)	SISM (2.0 fs)	SISM-MTS (2.0 fs)	Expt.
r_{OO_1} (Å)	2.8	2.8	2.8	2.88
$g_{OO}(r_{OO_1})$	2.75	2.77	2.75	3.09
r_{OH_1} (Å)	1.8	1.8	1.8	1.85
$g_{OH}(r_{OH_1})$	1.26	1.26	1.24	1.39
r_{HH_1} (Å)	2.5	2.5	2.5	2.45
$g_{HH}(r_{HH_1})$	1.21	1.21	1.21	1.26

MTS with $\delta t = 0.5$ fs for the integration of motions generated by high-frequency anharmonic interactions is less accurate than the SISM [Fig. 2(a)].

The error in total energy for the LFV-EQ, SISM-EQ, and SISM-MTS-EQ (Ref. 21) is depicted in Fig. 2(b). The total energy is defined in this case as[21]

$$H = T(\mathbf{p}) + V_{vib}(\mathbf{q}) + V_{nb}[\mathbf{d}(\mathbf{q})], \tag{21}$$

where $\mathbf{d}(\mathbf{q}) \in \mathbb{R}^{3n}$ are the equilibrium positions of atoms in all molecules of the system, given by the standard theory of molecular vibrations.[21,39–41] Since the vibrational potential V_{vib} used in the LFV-EQ is the same as in the LFV, the estimated value of the maximal acceptable time step for the LFV-EQ is also 0.5 fs.

From the results presented in Fig. 2(b) we can see that the error in total energy for the LFV-EQ with a 0.5 fs integration time step corresponds to the error for the SISM-EQ with a 2.0 fs integration time step and 3.0 fs for the SISM-MTS-EQ. The SISM-EQ therefore allows the use of a four times longer integration time step than the LFV-EQ for the same level of accuracy, whereas the SISM-MTS-EQ allows the use of even up to six times longer time steps than the LFV-EQ. The energy drift for integration time step's sizes longer than 3.0 fs is due to nonlinear instabilities, which occur when the integration step size is a third of the period of the fastest motion in the system as explained in Ref. 38.

The analytical solution of the equations of motion does not exist and the difference between trajectories calculated with different sizes of integration time steps and/or different integrators grows exponentially with time.[1] Therefore the accuracy of trajectories calculated by the new methods can not be checked by direct comparison of the calculated trajectories to the corresponding trajectories computed by the standard methods. Statistical correctness of the trajectories computed by the new methods can only be checked by computing different structural and dynamical properties of the molecular system and comparing them with corresponding properties calculated by the standard methods.

A. Structural properties

1. Radial distribution functions

The structure of the system of water molecules was checked by calculating site-site radial distribution functions $g_{OO}(r)$ for oxygens, $g_{OH}(r)$ for oxygens and hydrogens in different water molecules, and $g_{HH}(r)$ for hydrogens in different water molecules. The $g_{OO}(r)$, $g_{OH}(r)$, and $g_{HH}(r)$ were computed by the LFV, SISM, SISM-MTS, and LFV-EQ, SISM-EQ, and SISM-MTS-EQ from 100 ps long trajectories of the system of 256 flexible TIP3P water molecules with $\rho = 1.0$ g/cm^3 at $T = 300$ K using different sizes of the integration time step. Radial distributions functions calculated by the LFV using a 0.5 fs integration time step has been taken as a reference for the corresponding functions calculated by the SISM and SISM-MTS, whereas the radial distribution functions calculated by the LFV-EQ using a 0.5 fs integration time step have been taken as a reference for the corresponding functions obtained by the SISM-EQ and SISM-MTS-EQ. The positions and heights of the first maximum of $g_{OO}(r)$, $g_{OH}(r)$, and $g_{HH}(r)$, which are in good agreement with the published calculated results in the literature,[25,37] are given in Table III. The results reported in Table III show a good agreement between radial distribution functions calculated by the SISM and SISM-MTS using a 2.0 fs integration time step and the corresponding reference functions. The level of agreement with the experimental results depends mostly on the applied model of the water molecule and the "cut-off" function and not on the applied numerical integrator and/or the length of the integration time step.[42]

Since the site-site radial distribution functions are mostly force field dependent, they can be used to check the effect of the calculation of the electrostatic and van der Waals potentials in the equilibrium positions of the atoms as in the LFV-EQ, SISM-EQ, and SISM-MTS-EQ. The positions and heights of the first maximum of $g_{OO}(r)$, $g_{OH}(r)$, and $g_{HH}(r)$ are given in Table IV for the LFV-EQ using a 0.5 fs integration time step and the SISM-EQ and SISM-MTS-EQ using a 3.0 fs integration time step. We can again report a good agreement of the radial distribution functions calculated by the SISM-EQ and SISM-MTS-EQ using a 3.0 fs integration time step with corresponding reference functions.

B. Dynamical properties

The motion of water molecules in bulk can be characterized by dynamical properties of an individual molecule such as the diffusion coefficient and the orientational time constants, which can be also determined by MD simulation.[24]

TABLE IV. Comparison of $g_{OO}(r)$, $g_{OH}(r)$, and $g_{HH}(r)$ calculated by the LFV-EQ, SISM-EQ, and SISM-MTS-EQ. We give the positions and heights of the first maximum of the calculated functions and the corresponding experimental values (Ref. 42).

	LFV-EQ (0.5 fs)	SISM-EQ (3.0 fs)	SISM-MTS-EQ (3.0 fs)	Expt.
r_{OO_1} (Å)	2.8	2.8	2.8	2.88
$g_{OO}(r_{OO_1})$	2.54	2.55	2.55	3.09
r_{OH_1} (Å)	1.9	1.9	1.9	1.85
$g_{OH}(r_{OH_1})$	1.07	1.07	1.07	1.39
r_{HH_1} (Å)	2.5	2.5	2.5	2.45
$g_{HH}(r_{HH_1})$	1.17	1.17	1.17	1.26

1. Diffusion coefficient

The calculated values of the diffusion coefficient by Eq. (1) using the LFV, SISM, and SISM-MTS are reported in Table V, and suggest that the description of translational motion of molecules is independent of the choice of the numerical method and/or the size of the integration time step. The diffusion coefficients calculated by different integrators and/or different sizes of the integration time step are in good agreement.

A similar conclusion holds for the obtained diffusion coefficients using the LFV-EQ, SISM-EQ, and SISM-MTS-EQ, which are reported in Table VI. The diffusion coefficient values are increased in comparison to the results reported in Table V according to results from Ref. 15. However, the calculated diffusion coefficients given in Table V are also approximately two times larger than the experimental value. This is in accordance with the values obtained from a similar MD simulation in Ref. 37. The disagreement between calculated and experimental diffusion coefficients is due to the water model and not due to the applied numerical integrator. Good agreement between calculated diffusion coefficients obtained by different integrators is expected since all of them treat the molecules' translational degrees of freedom in the same way.

The calculated values of the diffusion coefficient obtained by virtue of Eq. (3) using different integrators and different sizes of the integration time step are reported in Tables V and VI. The obtained values are in good agreement with the values calculated by using Eq. (1). From the obtained results we can conclude that the translational motion of water molecules is correctly described by the SISM and its derivatives.

2. Orientational correlation times

The correlation times τ_l^α determined by Eqs. (4) and (5) using the LFV, SISM, and SISM-MTS using different sizes of the integration time step are reported in Table VII. The results obtained by different integrators are in good agreement for all sizes of integration time steps. This proves that the rotational motion of water molecules is also correctly described by the SISM and SISM-MTS using a 2.0 fs integration time step. The values of the calculated orientational correlation times given in Table VII are lower than the experimental values, which is in accordance with the results from similar calculations reported in the literature.[2,24,25] Despite that the experimental data suggests the rotation of a single water molecule in a bulk system is isotropic,[25,43] the obtained correlation times $\tau_l^\perp$ calculated by all numerical methods are shorter than τ_l^{HH} and τ_l^μ, which was also found by other authors.[25]

Similar conclusions are also valid for the results obtained using the LFV-EQ, SISM-EQ, and SISM-MTS-EQ, which are reported in Table VIII. From the results in Table VIII we can conclude that the rotation of a water molecule is correctly described by the SISM-EQ and SISM-MTS-EQ even with a 3.0 fs long integration time step.

Comparing the results in Tables VII and VIII we can observe that the values of τ_l^α are lower when the equilibrium

TABLE V. Diffusion coefficient D for the system of 256 flexible TIP3P water molecules calculated using Eq. (3) (MSD) and Eq. (1) (VAC) and various integration time steps. Experimental value of D for liquid water at $T=300$ K is 2.4×10^{-9} m^2/s (Ref. 37).

	[a] $\frac{D}{10^{-9}}$ (m^2/s)		[b] $\frac{D}{10^{-9}}$ (m^2/s)		[c] $\frac{D}{10^{-9}}$ (m^2/s)	
Δt (fs)	MSD	VAC	MSD	VAC	MSD	VAC
0.5	4.5	4.6	4.5	4.5	4.7	4.7
1.0	4.4	4.4	4.6	4.5	4.6	4.6
1.5	4.8	4.9	4.5	4.6	4.6	4.8
2.0	4.9	5.0	4.6	4.8	4.5	4.6

[a]Calculated by LFV.
[b]Calculated by SISM.
[c]Calculated by SISM-MTS.

TABLE VI. Diffusion coefficient D for the system of 256 flexible TIP3P water molecules calculated using Eq. (3) (MSD) and Eq. (1) (VAC) and various integration time steps. Experimental value of D for liquid water at $T=300$ K is 2.4×10^{-9}m^2/s (Ref. 37).

	[a] $\frac{D}{10^{-9}}$ (m^2/s)		[b] $\frac{D}{10^{-9}}$ (m^2/s)		[c] $\frac{D}{10^{-9}}$ (m^2/s)	
Δt (fs)	MSD	VAC	MSD	VAC	MSD	VAC
0.5	6.3	6.3	6.4	6.5	6.4	6.4
1.0	6.6	6.6	6.4	6.3	6.4	6.4
1.5	6.7	6.7	6.6	6.7	6.4	6.7
2.0	6.7	7.1	6.5	6.5	6.5	6.7
2.5	6.6	6.4	6.4	6.8	6.8	6.9
3.0	⋯	⋯	6.3	6.6	6.8	7.1

[a]Calculated by LFV-EQ.
[b]Calculated by SISM-EQ.
[c]Calculated by SISM-MTS-EQ.

positions of atoms are used to calculate the electrostatic and van der Waals potential energies. Comparing the diffusion coefficient given in Tables V and VI and relaxation times τ_1^μ for the dipole moment reported in Tables VII and VIII we see that shorter τ_1^μ, when calculating the electrostatic and van der Waals potential energies with atoms' equilibrium positions, are associated with larger diffusion coefficients. This is because the overall motion in liquid water is governed by the coupled translational and rotational motions of water molecules within first hydration shell.[24] If we calculate the product $(6D\tau_1^\mu)^{1/2}$ from corresponding data in Tables V–VIII, we obtain the value of 2.5Å for the average displacement independently from the manner of calculating the electrostatic and van der Waals potential energies. These values correspond to the average distance between two water molecules,[24] which are equal for both examples as can be seen from the results in Tables III and IV.

C. IR spectrum

The vibrational and rotational motions of molecules are those which involve energies that produce the spectra in the infrared region. Therefore, our newly developed MD integration methods are particulary suitable for computing the IR spectra because rotational, translational, and vibrational motions are resolved analytically, independent of the MD integration time step.

The IR spectra calculated by Eq. (10) of bulk water at $T=300$ K using the LFV, SISM, and SISM-MTS with integration time steps of lengths from 0.5 fs to 2.0 fs are shown in Figs. 3 and 4.

Figure 3(a) demonstrates that the IR spectra calculated by different numerical integrators using a 0.5 fs integration time step are in good agreement. These IR spectra were taken as a reference for comparison with calculated IR spectra using longer integration time steps. The magnitudes of the

TABLE VII. Orientational correlation times τ_l^α for the system of 256 flexible TIP3P water molecules at $T=300$ K obtained by using various integration time steps. The corresponding experimental values of τ_l^α at $T=300$ K are $\tau_2^{HH}=2.1$ ps (Ref. 48), $\tau_1^\mu=7.5$ ps (Ref. 24), $\tau_2^\perp=2.4$ ps (Ref. 43).

		[a] τ_l^α (ps)		[b] τ_l^α (ps)		[c] τ_l^α (ps)	
Δt	α	$l=1$	$l=2$	$l=1$	$l=2$	$l=1$	$l=2$
	HH	1.7	0.9	1.6	0.8	1.6	0.8
0.5	μ	2.3	0.9	2.2	0.9	2.2	0.8
	$\perp$	1.3	0.7	1.3	0.7	1.3	0.7
	HH	1.6	0.9	1.7	0.9	1.6	0.8
1.0	μ	2.2	0.9	2.2	0.9	2.2	0.8
	$\perp$	1.3	0.7	1.3	0.7	1.3	0.6
	HH	1.6	0.8	1.6	0.8	1.6	0.8
1.5	μ	2.1	0.8	2.1	0.8	2.2	0.9
	$\perp$	1.2	0.6	1.3	0.6	1.3	0.6
	HH	1.5	0.8	1.7	0.9	1.6	0.8
2.0	μ	2.1	0.8	2.2	0.9	2.2	0.9
	$\perp$	1.2	0.6	1.3	0.7	1.3	0.6

[a]Obtained by LFV.
[b]Obtained by SISM.
[c]Obtained by SISM-MTS.

TABLE VIII. Orientational correlation times τ_l^α for the system of 256 flexible TIP3P water molecules at $T=300$ K obtained by using various integration time steps. The corresponding experimental values of τ_l^α at $T=300$ K are $\tau_2^{\mathrm{HH}}=2.1$ ps (Ref. 48), $\tau_1^\mu=7.5$ ps (Ref. 24), $\tau_2^\perp=2.4$ ps (Ref. 43).

		[a]τ_l^α (ps)		[b]τ_l^α (ps)		[c]τ_l^α (ps)	
Δt	α	$l=1$	$l=2$	$l=1$	$l=2$	$l=1$	$l=2$
	HH	1.2	0.6	1.2	0.6	1.2	0.6
0.5	μ	1.5	0.6	1.6	0.6	1.5	0.6
	$\perp$	0.9	0.5	0.9	0.5	0.9	0.5
	HH	1.2	0.6	1.1	0.6	1.2	0.6
1.0	μ	1.5	0.6	1.4	0.6	1.5	0.6
	$\perp$	0.9	0.5	0.9	0.5	0.9	0.5
	HH	1.2	0.6	1.2	0.6	1.2	0.6
1.5	μ	1.5	0.6	1.5	0.6	1.5	0.6
	$\perp$	0.9	0.5	0.9	0.5	0.9	0.5
	HH	1.1	0.6	1.2	0.6	1.2	0.6
2.0	μ	1.4	0.6	1.5	0.6	1.5	0.6
	$\perp$	0.8	0.4	0.9	0.5	0.9	0.5
	HH	1.1	0.6	1.2	0.6	1.2	0.6
2.5	μ	1.4	0.6	1.5	0.6	1.5	0.6
	$\perp$	0.9	0.5	0.9	0.5	0.9	0.5
	HH	⋯	⋯	1.2	0.6	1.1	0.6
3.0	μ	⋯	⋯	1.5	0.6	1.5	0.6
	$\perp$	⋯	⋯	0.9	0.5	0.9	0.5

[a]Obtained by LFV-EQ.
[b]Obtained by SISM-EQ.
[c]Obtained by SISM-MTS-EQ.

spectral peaks were scaled so that the intensities of the higher peak positioned above the frequency of 3300 cm^{-1} and the stretching peak at 3408 cm^{-1} in the experimental spectrum are equal. The double peak at 3300 cm^{-1} corresponds to the normal modes of vibration of a water molecule describing the antisymmetric and symmetric bond stretches (see Table II). The single peak at 1775 cm^{-1} corresponds to the angle bending normal mode of a water molecule (see Table II). The IR band between 300 cm^{-1} and 900 cm^{-1} arises from to the librational motion of water molecules.[2]

When using a 1.0 fs integration time step, the high-frequency double peak at 3300 cm^{-1} in the IR spectrum calculated by the LFV already shifts to the higher frequencies as shown in Fig. 3(b). The observed blueshift suggests that when using a 1.0 fs integration time step, the LFV can no longer accurately describe the high-frequency vibrational motions of atoms in a water molecule, which has been already predicted by estimating the integration time step size from the error in the total energy shown in Fig. 2(a). This phenomenom is even more evident in Fig. 4 for the cases of

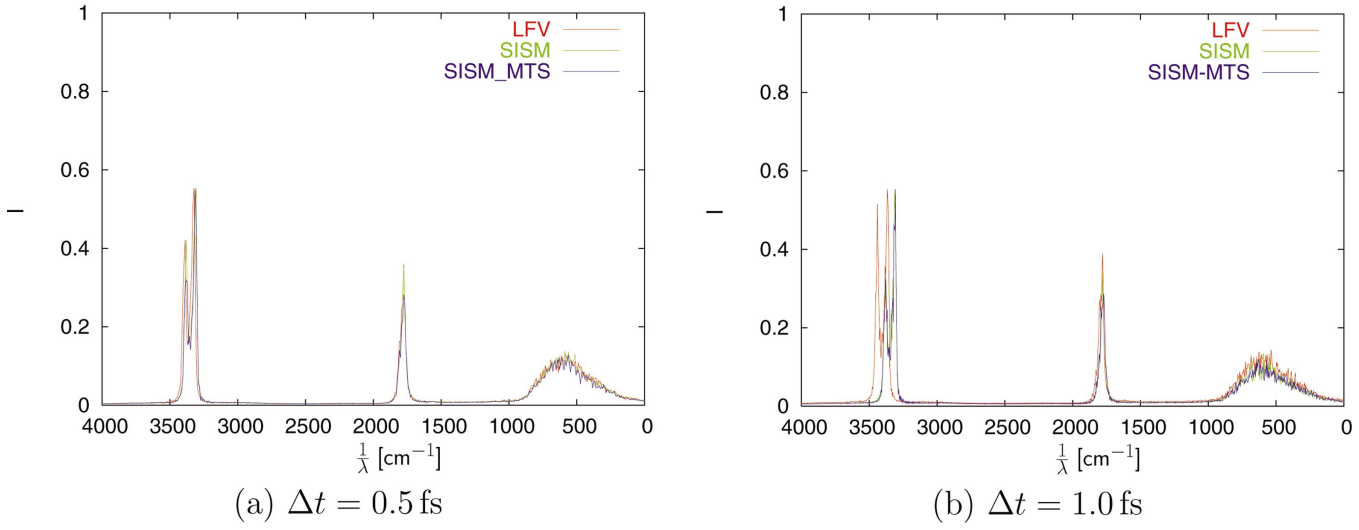

FIG. 3. (Color) IR spectrum (arbitrary units) of bulk water at $T=300$ K calculated by LFV, SISM, and SISM-MTS using an integration time step of (a) 0.5 fs and (b) 1.0 fs.

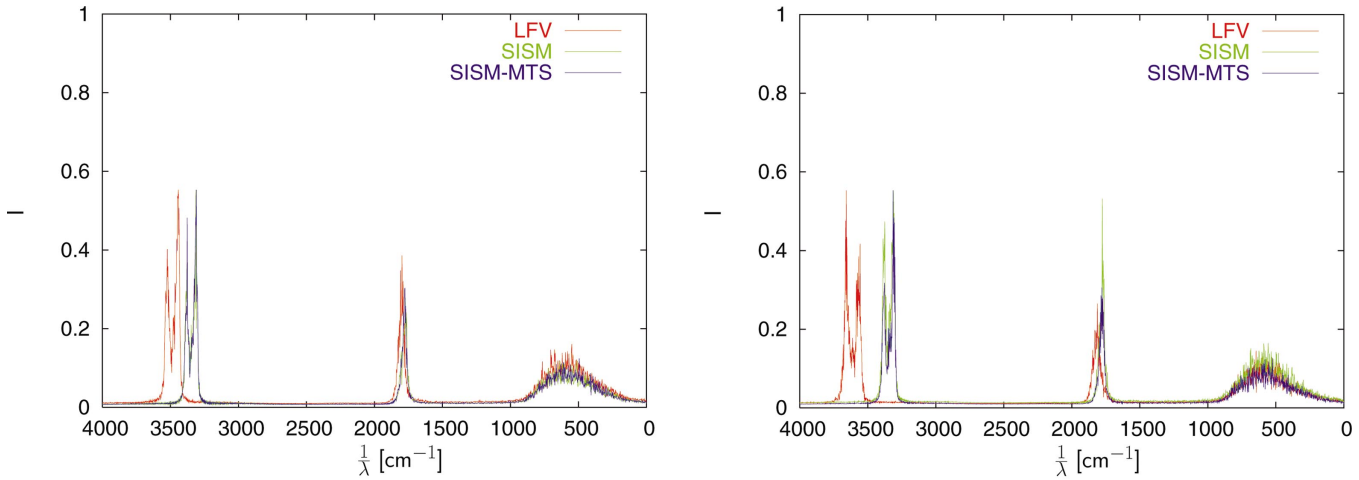

FIG. 4. (Color) IR spectrum (arbitrary units) of bulk water at $T=300$ K calculated by LFV, SISM, and SISM-MTS using an integration time step of (a) 1.5 fs and (b) 2.0 fs.

1.5 fs and 2.0 fs integration time steps where the peak at 1775 cm^{-1} also starts shifting toward higher frequencies. Peaks in corresponding IR spectra, which are calculated by the SISM and SISM-MTS, however, remain at the same positions as corresponding peaks in the reference IR spectra calculated using the integration time step of 0.5 fs. This proves that owing to the analytical description of high-frequency molecular vibrations, the later are accurately described by the SISM and SISM-MTS also using a 2.0 fs integration time step.

Comparing the results in Fig. 5(a), in which the calculated IR spectra of bulk water are shown calculated by the LFV-EQ, SISM-EQ, and SISM-MTS-EQ using a 2.5 fs integration time step, with those in Fig. 3(a) we can see that the peaks corresponding to the bond stretching and angle bending have remained in the same positions in IR spectra computed by the SISM-EQ and SISM-MTS-EQ. This is because the electrostatic and van der Waals interactions are not calculated between the atoms belonging to the same water molecule. The intensity of the band corresponding to the librational motion of water molecules is, however, slightly decreased in comparison with the IR spectrum in Fig. 3(a). Again, a blueshift of the the double peak at 3300 cm^{-1} can be observed in IR spectrum computed by the LFV-EQ. Therefore we can conclude that the LFV-EQ is also not able to accurately describe the high-frequency molecular vibrations using integration time steps longer than 0.5 fs. On the contrary, the IR spectra computed by the SISM-EQ and SISM-MTS-EQ show that these methods accurately describe high-frequency molecular vibrations even when using up to a 3.0 fs integration time step as can be observed from Fig. 5(b).

The calculated IR spectra as well as diffusion coefficients and rotational correlation times prove that the SISM and SISM-MTS correctly describe the translational, rotational, and vibrational degrees of freedom of water molecules up to a 2.0 fs integration time step. The error in total energy, however, shows that the size of the maximal allowed

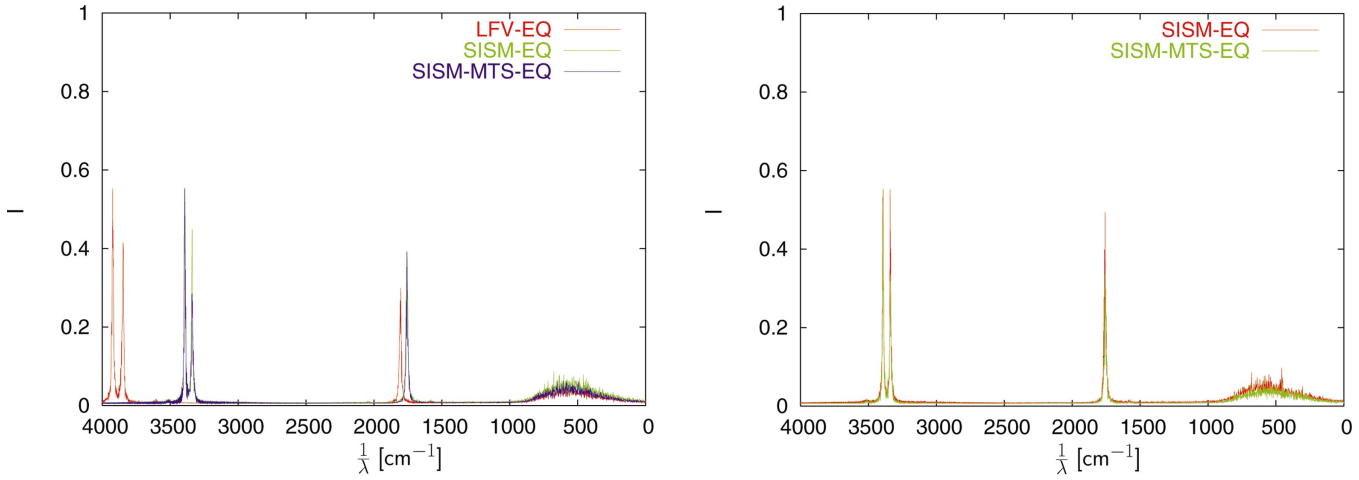

FIG. 5. (Color) IR spectrum (arbitrary units) of bulk water at $T=300$ K calculated by LFV-EQ, SISM-EQ, and SISM-MTS-EQ using an integration time step of (a) 2.5 fs and (b) 3.0 fs.

integration time step is 1.25 fs for the SISM and SISM-MTS in comparison with 0.5 fs for the LFV. From the computed data one can also conclude that the SISM-EQ and SISM-MTS-EQ also correctly integrate the translational, rotational, and vibrational motion of water molecules even up to a 3.0 fs integration time step. However, the error in total energy shows that the size of the maximal acceptable integration time step is 2.0 fs for the SISM-EQ and 3.0 fs in the example of the SISM-MTS-EQ, which is a sixfold speed-up in comparison with LFV-EQ.

V. CONCLUSIONS

We have presented a number of MD simulation of liquid water using newly introduced symplectic MD integrators which combine MD integration with the standard theory of molecular vibrations.[39–41] The computed structural and dynamical properties of the studied systems are in good agreement with the corresponding properties computed by the LFV using an accordingly short integration time step. Due to the analytical treatment of high-frequency molecular vibrations, the new methods are especially efficient for computing IR spectra since no blueshifting of the bond stretching normal mode peaks occurs, as is the case when using the LFV integrator. We also point out the ability of using a 3.0 fs integration time step with the SISM-MTS-EQ integration method at the same accuracy as employing the standard LFV method with a 0.5 fs integration time step. This is a sixfold simulation speed-up compared to the standard method for the simulation of a bulk water system.

We believe that new integration methods could become a method of choice in spectroscopic calculations[31,44–46] where the standard theory of molecular vibrations is applied to analyze the dynamics of the studied system from already computed MD trajectories. With our methods the information about the energy distribution of normal modes and the energy transfer between them is obtained without additional computations as opposed to the standard MD integration methods because the normal mode dynamics is computed along with the computation of the trajectory of a molecular system.

ACKNOWLEDGMENTS

The authors thank Dr. M. Hodošček and Dr. F. Merzel for helpful discussions and to U. Borštnik for careful reading of the manuscript. This work was supported by the Ministry of Education, Science and Sports of Slovenia under Grant Nos. P1-0002 and J1-6331.

[1] M. P. Allen and D. J. Tildesley, *Computer Simulation of Liquids* (Clarendon, Oxford, 1987).
[2] R. W. Impey, P. A. Madden, and I. R. McDonald, Mol. Phys. **46**, 513 (1982).
[3] J. Marti, J. Chem. Phys. **110**, 6876 (1999).
[4] A. Luzar, J. Chem. Phys. **113**, 10663 (2000).
[5] M. Boero, K. Terakura, T. Ikeshoji, C. Liew, and M. Parrinello, Phys. Rev. Lett. **85**, 3245 (2000).
[6] B. L. de Groot and H. Grubmuller, Science **294**, 2353 (2001).
[7] F. Merzel and J. C. Smith, Proc. Natl. Acad. Sci. U.S.A. **99**, 5378 (2002).
[8] M. Matsumoto, S. Saito, and I. Ohmine, Nature (London) **416**, 409 (2002).
[9] Ph. Wernet, D. Nordlund, U. Bergmann, M. Cavalleri, M. Odelius, H. Ogasawara, L. A. Naslund, T. K. Hirsch, L. Ojamäe, P. Glantzel, L. G. M. Pettersson, and A. Nilsson, Science **304**, 995 (2004).
[10] J. P. Ryckaert, G. Ciccotti, and H. J. C. Berendsen, J. Comput. Phys. **23**, 327 (1977).
[11] H. C. Anderson, J. Comput. Phys. **52**, 24 (1983).
[12] M. E. Tuckerman, G. J. Martyna, and B. J. Berne, J. Chem. Phys. **93**, 1287 (1990).
[13] M. E. Tuckerman, B. J. Berne, and G. J. Martyna, J. Chem. Phys. **97**, 1990 (1992).
[14] B. Garcia-Archilla, J. M. Sanz-Serna, and R. D. Skeel, SIAM J. Sci. Comput. (USA) **20**, 930 (1998).
[15] J. A. Izaguirre, S. Reich, and R. D. Skeel, J. Chem. Phys. **110**, 9853 (1999).
[16] R. D. Skeel and J. A. Izaguirre, in *Computational Molecular Dynamics: Challenges, Methods, Ideas*, Lecture Notes in Computational Science and Engineering, Vol. 4, edited by P. Deuflhard, J. Hermans, B. Leimkuhler, A. E. Mark, S. Reich, and R. D. Skeel (Springer, Berlin, 1999).
[17] L. Verlet, Phys. Rev. **159**, 98 (1967).
[18] W. L. Jorgensen, J. Chandrasekhar, J. D. Madura, R. W. Impey, and M. L. Klein, J. Chem. Phys. **79**, 926 (1983).
[19] P. J. Steinbach and B. R. Brooks, J. Comput. Chem. **15**, 667 (1994).
[20] A. R. Leach, *Molecular Modelling*, 2nd ed. (Pearson, Harlow, 2001).
[21] D. Janežič, M. Praprotnik, and M. Merzel, J. Chem. Phys. **122**, 174101 (2005), this issue.
[22] J. M. Sanz-Serna and M. P. Calvo, *Numerical Hamiltonian Problems* (Chapman & Hall, London, 1994).
[23] A. R. Leach, *Molecular Modelling*, 2nd ed. (Pearson, Harlow, 2001).
[24] A. Wallqvist and B. J. Berne, J. Phys. Chem. **97**, 13841 (1993).
[25] D. van der Spoel, P. J. van Maaren, and H. J. C. Berendsen, J. Chem. Phys. **108**, 10220 (1998).
[26] W. H. Press, B. P. Flannery, S. A. Teukolsky, and W. T. Vetterling, *Numerical Recipes: The Art of Scientific Computing* (Cambridge University Press, Cambridge, 1987).
[27] B. Guillot, J. Chem. Phys. **95**, 1543 (1991).
[28] B. Borštnik, D. Pumpernik, D. Janežič, and A. Ažman, in *Molecular Interactions*, edited by H. Ratajczak and W. J. Orville-Thomas (Wiley, 1980).
[29] B. Boulard, J. Kieffer, C. C. Phifer, and C. A. Angell, J. Non-Cryst. Solids **140**, 350 (1992).
[30] P. Bornhauser and D. Bougeard, J. Phys. Chem. B **105**, 36 (2001).
[31] M. Praprotnik, D. Janežič, and J. Mavri, J. Phys. Chem. A **108**, 11056 (2004).
[32] D. Janežič and B. R. Brooks, J. Comput. Chem. **16**, 1543 (1995).
[33] M. Praprotnik and D. Janežič, J. Chem. Phys. **122**, 174102 (2005), preceding paper.
[34] L. D. Landau and E. M. Lifshitz, *Course of Theoretical Physics: Mechanics*, 3rd ed. (Pergamon, Oxford, 1976), Vol. 1.
[35] G. A. Natanson, Chem. Phys. Lett. **121**, 343 (1985).
[36] C. L. Brooks III, B. M. Pettitt, and M. Karplus, J. Chem. Phys. **83**, 5897 (1985).
[37] M. Prevost, D. van Belle, G. Lippens, and S. Wodak, Mol. Phys. **71**, 587 (1990).
[38] Q. Ma, J. A. Izaguirre, and R. D. Skeel, SIAM J. Sci. Comput. (USA) **24**, 1951 (2003).
[39] C. Eckart, Phys. Rev. **47**, 552 (1935).
[40] E. B. Wilson, J. C. Decius, and P. C. Cross, *Molecular Vibrations* (McGraw-Hill, New York, 1955).
[41] J. D. Louck and H. W. Galbraith, Rev. Mod. Phys. **48**, 69 (1976).
[42] A. K. Soper and M. G. Phillips, Chem. Phys. **107**, 47 (1986).
[43] B. Halle and H. Wennerström, J. Chem. Phys. **75**, 1928 (1981).
[44] R. Rey, J. Chem. Phys. **104**, 2356 (1996).
[45] R. Rey, Chem. Phys. **229**, 217 (1998).
[46] R. Rey, J. Chem. Phys. **108**, 142 (1998).
[47] *Handbook of Chemistry and Physics*, edited by D. Lide (CRC, Boca Raton, FL, 1995).
[48] J. Jonas, T. DeFries, and D. J. Wilbur, J. Chem. Phys. **65**, 582 (1976).